Received August 16, 2020, accepted August 30, 2020, date of publication September 4, 2020, date of current version September 18, 2020.

Digital Object Identifier 10.1109/ACCESS.2020.3021798

Influence of Thermal Aging on Space Charge Accumulation and Dissipation of Cross-Linked Polyethylene With Different Cross-Linking Agent Contents

SHUCHAO WANG[1], QUAN ZHOU[1], JIAN LI[1], (Senior Member, IEEE), RUIJIN LIAO[1], NENGCHENG WU[2], YONG LI[1], AND MINGHAO CHEN[1]

[1]State Key Laboratory of Transmission and Distribution Equipment and Power System Safety and New Technology, School of Electrical Engineering, Chongqing University, Chongqing 400044, China

[2]Deyang Electric Power Supply Company, State Grid Corporation, Deyang 618000, China

Corresponding author: Quan Zhou (cqzhouquan@163.com)

This work was supported in part by the National Key Research and Development Program of China under Grant 2017YFB0902300, and in part by the Project 111 of the Ministry of Education of China under Grant B08036.

ABSTRACT This article presents the influence of thermal aging on space charge accumulation and dissipation of cross-linked polyethylene (XLPE) with different cross-linking agent contents. In this article, dicumyl peroxide (DCP) and low-density polyethylene (LDPE) respectively are used as cross-linking agent and basic experimental material. Additionally, an improved PEA method is used to measure space charge densities during voltage application and removal when thermal aging time respectively is 0, 5, 15, 30 and 80 days due to higher accuracy. And experimental results indicate thermal aging can introduce negative charge traps into pure LDPE and make space charges easier to inject and accumulate in pure LDPE and XLPE, but space charge densities in XLPE increase more rapidly as thermal aging time increases, moreover, thermal aging can simultaneously increase densities of deep and shallow charge traps in pure LDPE and XLPE, etc. And we have also explained the change of space charge accumulation and dissipation of pure LDPE and XLPE after thermal aging from the perspective of micro-structure change of pure LDPE and XLPE through the quantitative analysis of average charge densities. Besides, theoretical model of the average charge decay has also been summed up, and this model can perfectly reflect the dissipation of space charges in pure LDPE and XLPE of different thermal aging time.

INDEX TERMS Cross-linked polyethylene (XLPE), DCP content, improved pulsed electro-acoustic (PEA) method, low-density polyethylene (LDPE), thermal aging, space charge.

I. INTRODUCTION

Cross-linked polyethylene (XLPE) has been widely used as power cable insulation materials [1], [2]. Compared with traditional oil-paper-insulated cables, XLPE cables have many significant advantages such as high softening point, low thermal deformation, high mechanical strength at high temperature, light weight, acid resistance, alkali resistance, corrosion resistance, almost no cracking and so on [1]–[4]. Therefore, owing to these advantages, XLPE cables quickly conquered the power industry as soon as they came out.

The associate editor coordinating the review of this manuscript and approving it for publication was Ting Yang.

At present, many scholars all over the world have done a lot of research work on the modification of polyethylene materials and XLPE materials [2]–[16], such as heat treatment to eliminate cross-linking by-products, the introduction of additives to prevent the accumulation of space charges and so on [4]–[15]. However, most of the researches mainly focus on the simple description of macroscopic phenomena, and lack of in-depth analysis of microscopic reasons causing such macroscopic phenomena. Currently, few scholars have systematically studied the influence of thermal aging on space charge accumulation and dissipation of XLPE with different cross-linking agent contents, however, this is exactly the focus of this article.

As we know, any research team who wants to study space charges must measure space charges. Currently, there are many ways to measure space charges. For example, destructive measurement methods such as thermally stimulated current method, thermally stimulated surface potential method and thermoluminescence method, or nondestructive measurement methods such as Piezo-electric Induced Pressure Wave Propagation method, Laser Induced Pressure Propagation method and Pulsed Electro-Acoustic (PEA) method [17].

However, these methods all have their own problems [17]–[19]. Therefore, this article has used an improved PEA method to measure space charges for higher measurement accuracy. We have used space charge density data obtained by this improved PEA method to analyze the influence of thermal aging on space charge accumulation and dissipation of XLPE with different cross-linking agent contents. Besides, the average charge density has also been introduced into the experiment as characteristic parameter to quantitatively analyze the influence, and theoretical model of the average charge decay has also been summarized. In addition, we have used the average charge data to theoretically explain the influence of thermal aging on space charge accumulation and dissipation of XLPE with different cross-linking agent contents from a microscopic perspective. Finally, some very regular conclusions can be obtained and shown in this article.

II. MATERIALS AND METHODS

A. EXPERIMENTAL PREPARATION

In this experiment, basic experimental material is LDPE granules (Model: 2426H; Density distribution: 0.910–0.925 mg/mm^3; Melt index: 2.1–2.2; Melting point: 112 °). In addition, cross-linking agent is white DCP crystals (Molecular formula: $C_{18}H_{22}O_2$; Relative molecular mass: 270.37; Melting point: 41–42 °; Relative density: 1.082; Decomposition temperature: 120–125 °; Active oxygen content: 5.92% (DCP purity:100%), 5.62% (DCP purity: 95%); Stable at room temperature).

In addition, we have followed the reference [20] to prepare pure LDPE samples and XLPE samples with 1.0%, 2.1%, 3.0%, and 5.0% DCP. And the size of these samples was all 4 cm × 4 cm × approximate 160 μm.

And in order to eliminate the interference of heat stress, water vapor, acetophenone and other cross-linking by-products generated during sample preparation process [6], [16]. We have used the method of vacuum drying and degassing to pretreat the prepared samples, namely, these samples have been placed into a vacuum drying box (the temperature at 80 ° and the pressure at 50 Pa) to dry and degas for 48 hours.

B. ESTABLISHMENT OF LONG-TERM AGING SYSTEM

In order to study the influence of thermal aging on space charge accumulation and dissipation of XLPE with different cross-linking agent contents, it is necessary to eliminate oxidation interference of oxygen on samples during thermal aging. Therefore, we need to build a long-term thermal aging system in the laboratory.

We have put the prepared samples into a heat-resistant glass container and dried them in a vacuum oven (the temperature at 80 °C and the pressure at 50 Pa) for 24 hours before thermal aging. Then the glass container has been sealed after filling the vacuum drying oven with nitrogen to a standard atmospheric pressure. And then put all samples into a large beaker and put them together in a thermal aging chamber (the temperature at 90 °C) for long-term thermal aging. And thermal aging time has been set to 0, 5, 15, 30 and 80 days respectively. When thermal aging time has reached a certain number of days, a certain number of samples can be taken from the glass container for relevant experiments. At the same time, put the remaining samples into a vacuum drying oven, and then vacuum them and inject nitrogen into a standard atmosphere and repeat this three times to ensure no residual air in the glass container, and then seal the glass container and continue to place it in the thermal aging chamber. And the process can be repeated again until thermal aging experiments have been all over.

C. SPACE CHARGE MEASUREMENT

According to the principle of space charge density measurement on PEA method [17], it can be known that the factors affecting measurement results mainly are relative permittivity of a tested sample, propagation speed of sound wave in a tested sample, thickness of a tested sample, the applied DC electric field between two electrodes, the width of an electrical pulse applied to a tested sample, a reference signal and a measurement signal. And most of these influencing factors can be determined when these hardware measurement systems for space charges are determined, thus three factors affecting the test accuracy mainly are relative permittivity of a tested sample, propagation speed of sound wave in a tested sample and thickness of a tested sample [17], [18]. In current PEA method, relative permittivity and propagation speed of sound wave are given according to the type of these tested samples, and thickness value of a tested sample is calculated by a program written by propagation speed of sound wave in a tested sample and initial value of reference signal in time domain. In fact, relative permittivity and propagation speed of sound wave are often affected by many factors such as aging, sample purity, temperature, humidity and so on, and these factors can make actual relative permittivity and propagation velocity of sound wave very different from given values, which can greatly affect measurement accuracy of space charge density.

In order to obtain accurate space charge density, we have used space charge waveform recovery algorithm. In this algorithm, accurate relative permittivity of a tested sample is first obtained by actual measurement, and then actual propagation velocity of sound wave in a tested sample is calculated by actual thickness of a tested sample and reference signal value, finally, we have used accurate parameters to achieve

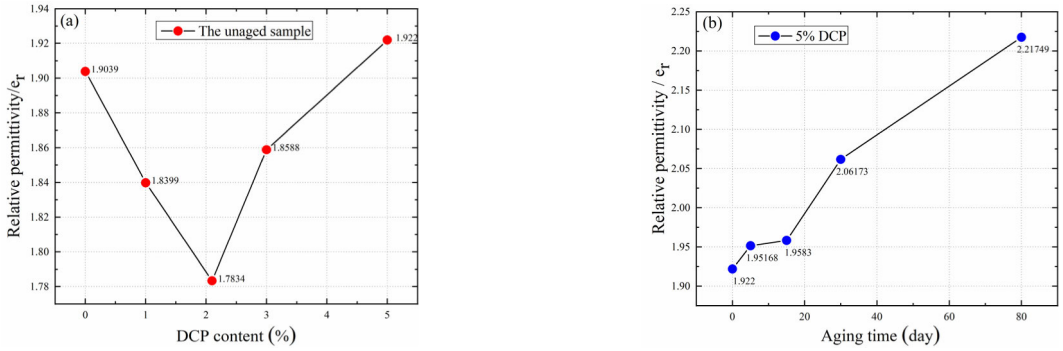

FIGURE 1. (a) Relative permittivity values at 50 Hz of unaged XLPE samples with different cross-linking agent contents. (b) Relative permittivity values at 50 Hz of XLPE samples with 5.0% DCP at different aging times.

accurate analysis of measurement data, which can be called an improved PEA method.

For this method, accurate relative permittivity of each sample needs to be obtained, thus Concept 80 Broadband Dielectric Spectrometer System has been used in this article. Relative permittivity, dielectric loss factor and other parameters of XLPE samples can be obtained through this system.

In the measurement system for space charges, the expression of space charge distribution in frequency domain can be as follows [17]–[20]

$$\left[\frac{\sigma_0}{v_{sa}\Delta\tau} + R(f) + \frac{\sigma_d}{v_{sa}\Delta\tau}\exp\left(-j2\pi f\frac{d}{v_{sa}}\right)\right] = \frac{V(f)}{S(f)} = \varepsilon_0\varepsilon_r\frac{V_{dc}}{d}\frac{1}{v_{sa}\Delta\tau}\frac{V(f)}{V_0(f)} \quad (1)$$

In (1), σ_0 and σ_d respectively represent space charge values induced on two electrodes in this test system. v_{sa} represents propagation speed of sound waves in a tested sample. V(f) represents this expression of measured voltage signals in frequency domain. $\Delta\tau$ represents the width of an electrical pulse applied to a tested sample. S(f) represents transfer function of the test system. ε_r represents relative permittivity of a tested sample. $V_0(f)$ represents the expression of reference voltage signals in frequency domain. V_{dc} represents DC electric field applied between two electrodes in the test system, and d represents thickness value of a tested sample.

Space charge density values can be obtained by substituting relative permittivity values at 50 Hz of these tested samples into (1). Figure 1 (a) shows relative permittivity values at 50 Hz of unaged XLPE samples with different cross-linking agent contents. It can be seen from Figure 1 (a) that relative permittivity values of unaged samples show a trend of decreasing first and then increasing as DCP content increases, and relative permittivity reaches the minimum when DCP content is 2.1%. Figure 1 (b) shows relative permittivity values at 50 Hz of XLPE samples with 5.0% DCP at different aging times. It can be seen from Figure 1 (b) that the relative permittivity gradually increases as thermal aging time increases.

Therefore, relative permittivity can be greatly affected by DCP content and thermal aging time. If actual situation of each experiment and each sample is not considered and a fixed relative permittivity value is always used, this can lead to introduce a large experimental error. Therefore, this does indicate this improved PEA method is necessary.

In addition, we also need to calculate accurate sound pulse velocity by reference signal (REF) and actual thickness of each sample. REF is a signal obtained by PEA detection when a lower voltage insufficient to cause space charges to accumulate inside the tested sample is applied to the tested sample. When 1 kV voltage is applied to pure LDPE sample with a thickness of 160 μm, and REF is shown in Figure 2 (a). Actual sampling frequency is 2.5 G/s and each data point corresponds to 0.4 ns. Then propagation time of sound pulse in the sample is 75.2 ns, thus propagation speed of sound wave is 2167.55 m/s. Figure 2 (b) shows sound velocity values of XLPE samples with different cross-linking agent contents. It can be seen from Figure 2 (b) that propagation velocity of sound wave gradually decreases as DCP content increases. Figure 2 (c) shows sound velocity values of XLPE samples with 3.0% DCP at different thermal aging time. It can be seen from Figure 2 (c) that propagation speed of sound pulse fluctuates within a certain range, and there is a large difference in sound velocity between specific samples.

Obviously, if the fixed value (2156 m/s) is still used for data processing without considering the change of sound velocity in the specific sample, the obtained space charge densities can have large errors. Thus accurate sound velocity value of each sample can be obtained by the above method.

In order to verify the necessity of the improved PEA method, here are two examples of data processing. The first example is REF data processing of an unaged sample with 2.1% DCP, and the second example is REF data processing of a sample with 5% DCP aged for 15 days.

Figure 3 (a) shows space charge densities before and after the correction for unaged samples with 2.1% DCP. Actual thickness values of those samples are all 160 μm, and actual relative permittivity ε_r is 1.7834, and the calculated sound pulse velocity v_{sa} is 2005.07 m/s, and the applied voltage is 1 kV. Additionally, the parameter ε_r of REF takes 2.3 and v_{sa} takes 2156 m/s, and the parameter ε_r of REF-1 takes 1.7834 and v_{sa} takes 2156 m/s, and the parameter ε_r of

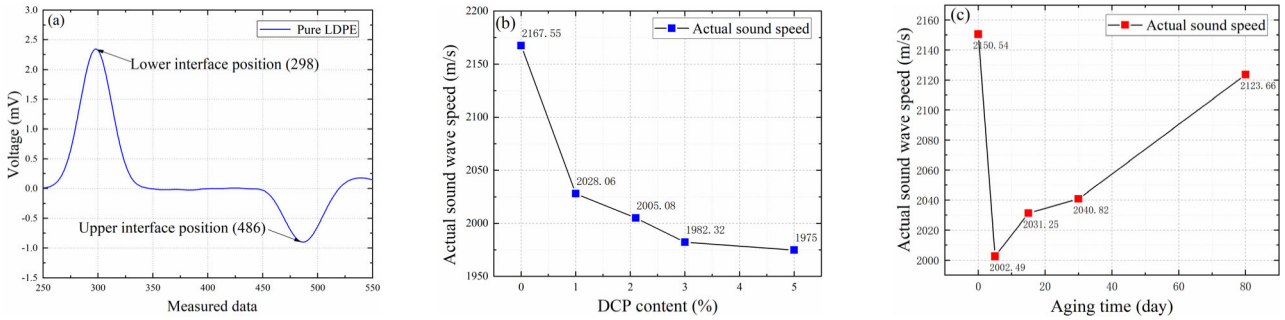

FIGURE 2. (a) Pure LDPE reference signal. (b) Sound velocity values of XLPE samples with different cross-linking agent contents. (c) Sound velocity values of XLPE samples with 3.0% DCP at different thermal aging times.

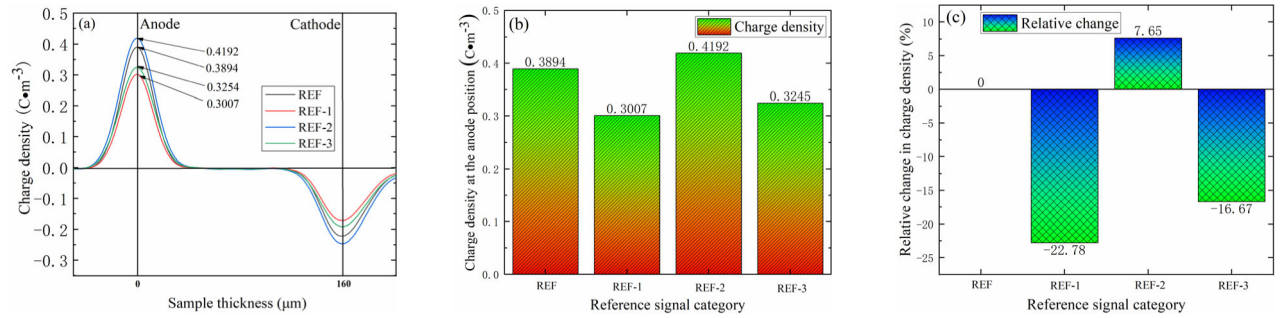

FIGURE 3. (a) Space charge densities before and after the correction for unaged samples with 2.1% DCP. (b) Space charge density value of each curve at anode in (a). (c) Variation of space charge density value of each curve at anode in (a) relative to that of REF in (a).

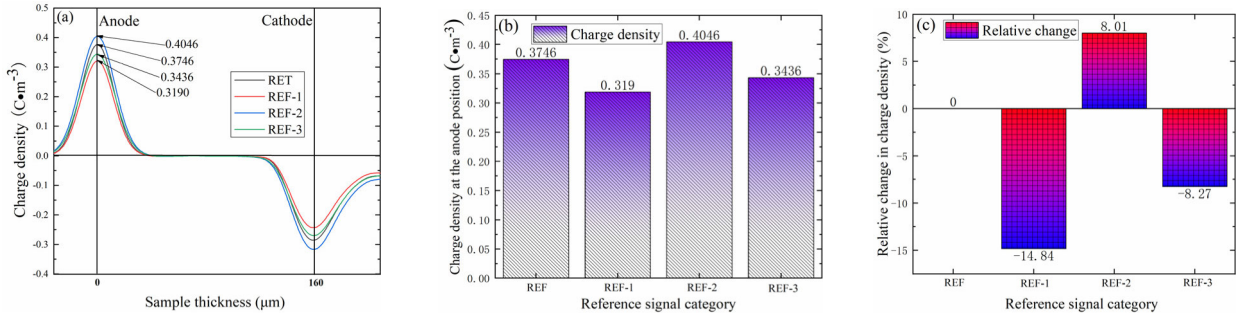

FIGURE 4. (a) Space charge densities before and after the correction of XLPE samples with 5.0% DCP aged for 15 days. (b) Space charge density value of each curve at anode in (a). (c) Variation of space charge density value of each curve at anode in (a) relative to that of REF in (a).

REF-2 takes 2.3 and v_{sa} takes 2005.07 m/s, and the parameter ε_r of REF-3 takes 1.7834 and v_{sa} takes 2005.07 m/s. Figure 3 (b) shows space charge density value of each curve at anode in Figure 3 (a). Figure 3 (c) shows variation of space charge density value of each curve at anode in Figure 3 (a) relative to that of REF in Figure 3 (a). It can be seen from Figure 3 (a), (b) and (c) that compared with uncorrected REF data, REF-1 is reduced by 22.78%, and REF-2 is increased by 7.65%, moreover, REF-3 is decreased by 16.67%, which indicates it is necessary to correct data.

It can be seen from Figure 3 (a), (b) and (c) combined with (1) that the obtained space charge density is reduced when only relative permittivity is corrected because actual relative permittivity is lower than the fixed value, and the obtained space charge density is increased when only sound pulse velocity is corrected because actual sound pulse velocity is lower than the fixed value. Theoretically, space charge densities obtained by simultaneously correcting relative permittivity and sound pulse velocity are the most accurate, thus in Figure 3 (a), only space charge density represented by REF-3 is the most accurate.

Figure 4 (a) shows space charge densities before and after the correction for XLPE samples with 5.0% DCP aged for 15 days. Actual thickness values of these samples are all 160 μm, and actual relative permittivity ε_r is 1.9583, and the calculated sound pulse velocity v_{sa} is 2010.05 m/s and the applied voltage is 1 kV. Additionally, the parameter ε_r of REF takes 2.3 and v_{sa} takes 2156 m/s, and the parameter

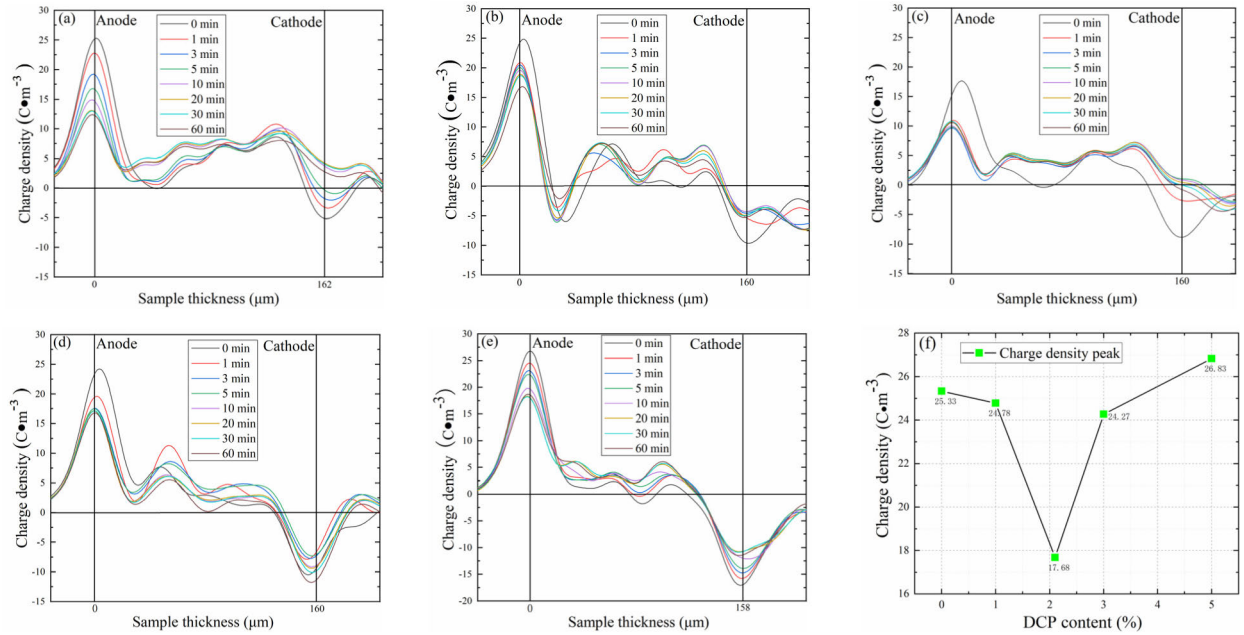

FIGURE 5. (a)-(e) Space charge density distributions of XLPE samples with different cross-linking agent contents in applied voltage experiment when thermal aging time is 0 days. (a) Pure LDPE. (b) 1.0% DCP. (c) 2.1% DCP. (d) 3.0% DCP. (e) 5.0% DCP. (f) Space charge density peak values at anode of XLPE samples with different cross-linking agent contents.

ε_r of REF-1 takes 1.9583 and v_{sa} takes 2156 m/s, and the parameter ε_r of REF-2 takes 2.3 and v_{sa} takes 2010.05 m/s, and the parameter ε_r of REF-3 takes 1.9583 and v_{sa} takes 2010.05 m/s. Figure 4 (b) shows space charge density value of each curve at anode in Figure 4 (a). Figure 4 (c) shows variation of space charge density value of each curve at anode in Figure 4 (a) relative to that of REF in Figure 4 (a). It can be seen from Figure 4 (a), (b) and (c) that compared with uncorrected REF data, REF-1 is reduced by 14.84%, and REF-2 is increased by 8.01%, moreover, REF-3 is decreased by 8.27%, which indicates it is necessary to correct data.

Therefore, it can be seen from the two examples that the obtained space charge densities can have large errors if space charge densities are not corrected or only a part is corrected, thus this improved PEA method is very necessary for the study of space charges.

D. EXPERIMENTAL METHODS

In order to study the influence of thermal ageing on space charge accumulation of XLPE samples with 0% DCP, 1.0% DCP, 2.1% DCP, 3.0% DCP and 5.0% DCP, the voltage was applied for one hour at 50 kV/mm, and the improved PEA test of applied voltage respectively was implemented at 0 min, 1 min, 3 min, 5 min, 10 min, 20 min, 30 min and 60 min.

In order to study the influence of thermal aging on space charge dissipation of XLPE samples with 0% DCP, 1.0% DCP, 2.1% DCP, 3.0% DCP and 5.0% DCP, the applied electric field of 50kV/mm was removed after applying the voltage for one hour, and the upper and lower electrodes were short-circuited and grounded. The improved PEA test of removed voltage respectively was performed at 0 min, 1 min, 2 min, 5 min, 10 min, and 20 min.

In order to more intuitively analyze the influence of thermal aging on space charge accumulation and dissipation of XLPE samples with 0% DCP, 1.0% DCP, 2.1% DCP, 3.0% DCP and 5.0% DCP, the measured space charge distribution needs to be quantitatively analyzed to extract relevant characteristic parameters of space charge distribution in voltage application and removal experiments. At the same time, since the average charge density excludes the influence of electrode cross-sectional area of this PEA test system and sample thickness, the average charge density q(t) can be used for further analysis [20].

$$q(t) = \frac{1}{d}\int_0^d \left|q_t(x,t)\right| dx \tag{2}$$

In (2), $q_t(x,t)$ represents space charge density at the position x of thickness direction of a tested sample at time t; d represents thickness value of a tested sample; q (t) represents the average density of space charges in a tested sample at time t.

III. RESULTS AND DISCUSSION

A. INFLUENCE OF THERMAL AGING ON SPACE CHARGE ACCUMULATION OF XLPE WITH DIFFERENT CROSS-LINKING CONTENTS

Figure 5 (a)-(e) shows space charge density distributions of XLPE samples with different cross-linking agent contents in applied voltage experiment when thermal aging time is 0 days. It can be seen from Figure 5 (a)-(e) that the peak value of space charge density at anode decreases first and

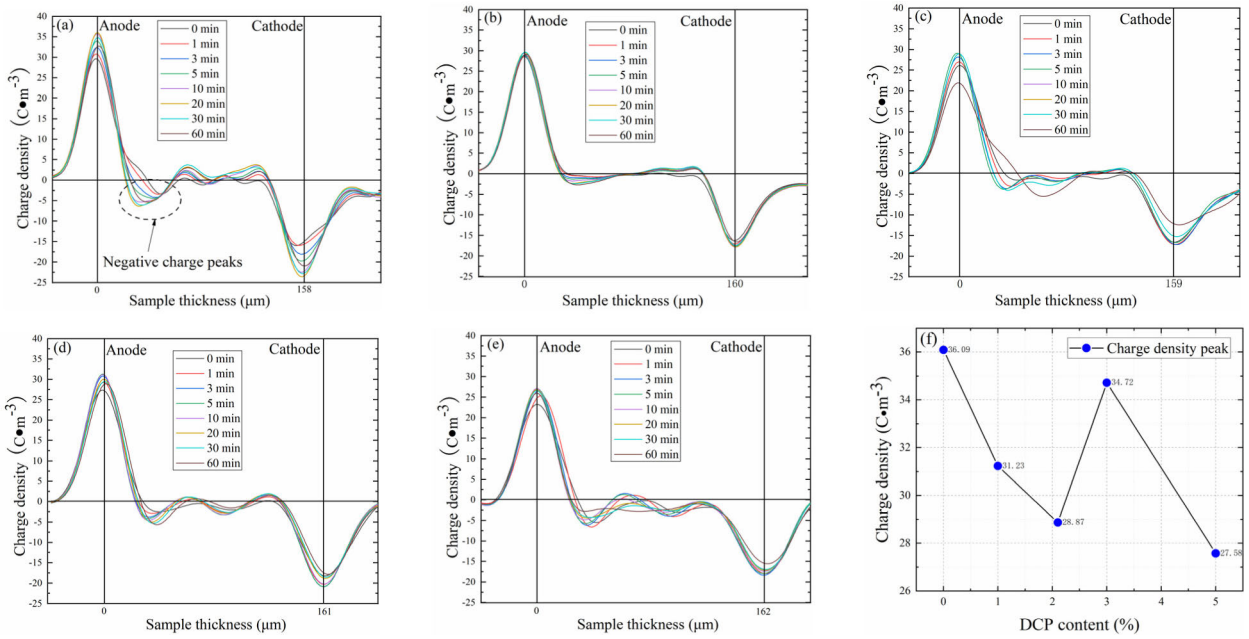

FIGURE 6. (a)-(e) Space charge density distributions of XLPE samples with different cross-linking agent contents in applied voltage experiment when thermal aging time is 5 days. (a) Pure LDPE. (b) 1.0% DCP. (c) 2.1% DCP. (d) 3.0% DCP. (e) 5.0% DCP. (f) Space charge density peak values at anode of XLPE samples with different cross-linking agent contents.

then increases as DCP content increases, and these values are shown in Figure 5 (f). It can be seen from Figure 5 (f) that the value of XLPE sample with 2.1% DCP is lowest.

Figure 6 (a)-(e) shows space charge density distributions of XLPE samples with different cross-linking agent contents in applied voltage experiment when thermal aging time is 5 days. Compared with space charge distributions of unaged samples, it can be found that space charge density values in these samples are greatly improved after thermal aging. It can be seen from Figure 6 (a)-(e) that pure LDPE sample has the largest charge densities at two electrodes, and space charge density inside pure LDPE sample is also the largest. Besides, the peak value of space charge density distribution of pure LDPE sample is 36.09 $C{\cdot}m^{-3}$, and the corresponding values of other samples are around 30 $C{\cdot}m^{-3}$, and these values are shown in Figure 6 (f).

Space charge distributions of these samples fluctuate less except for that of pure LDPE sample in applied voltage experiment, which shows space charge distributions in samples after cross-linking quickly reach equilibrium. Compared with space charge distributions of unaged samples, the accumulation of negative charges in pure LDPE sample near the anode has increased significantly and negative charge density peaks start to appear, which indicates thermal aging introduces negative charge traps into pure LDPE. Additionally, it can be clearly seen that negative charges move towards the anode and gradually accumulate near the anode, at the same time, positive charges move towards the cathode and gradually accumulate near the cathode.

Figure 7 (a)-(e) shows space charge density distributions of XLPE samples with different cross-linking agent contents in applied voltage experiment when thermal aging time is 15 days, and space charge density peak values of these samples at anode are shown in Figure 7 (f). It can be seen from Figure 7 (f) that the value is first decreased and then increased.

It can be seen from Figure 7 (a)-(e) that space charge values of pure LDPE sample at two electrodes and inside pure LDPE sample are the largest, while the number of charges in interior of XLPE samples is very small, which indicates space charges are injected and accumulated in pure LDPE easier, however, it is more difficult to inject and accumulate in XLPE. And similar to space charge distributions of samples aged for 5 days, there is an accumulation of negative charges near the anode in pure LDPE sample, and negative charge peaks start to appear.

Figure 8 (a)-(e) shows space charge density distributions of XLPE samples with different cross-linking agent contents in applied voltage experiment when thermal aging time is 30 days, and space charge density peak values at anode are shown in Figure 8 (f). It can be seen from Figure 8 (f) that the value is minimized when DCP content is 2.1%. It can be seen from Figure 8 (a)-(f) that the number of space charges accumulated inside pure LDPE is still the most and the charge density peak is also the largest, however, space charge density peak values inside XLPE samples are only slightly smaller than that of pure LDPE sample, what's more, some values are similar to that of pure LDPE sample, which indicates space charges are injected and accumulated in pure LDPE and XLPE easier, but space charge densities in XLPE samples increase more rapidly as thermal aging time increases.

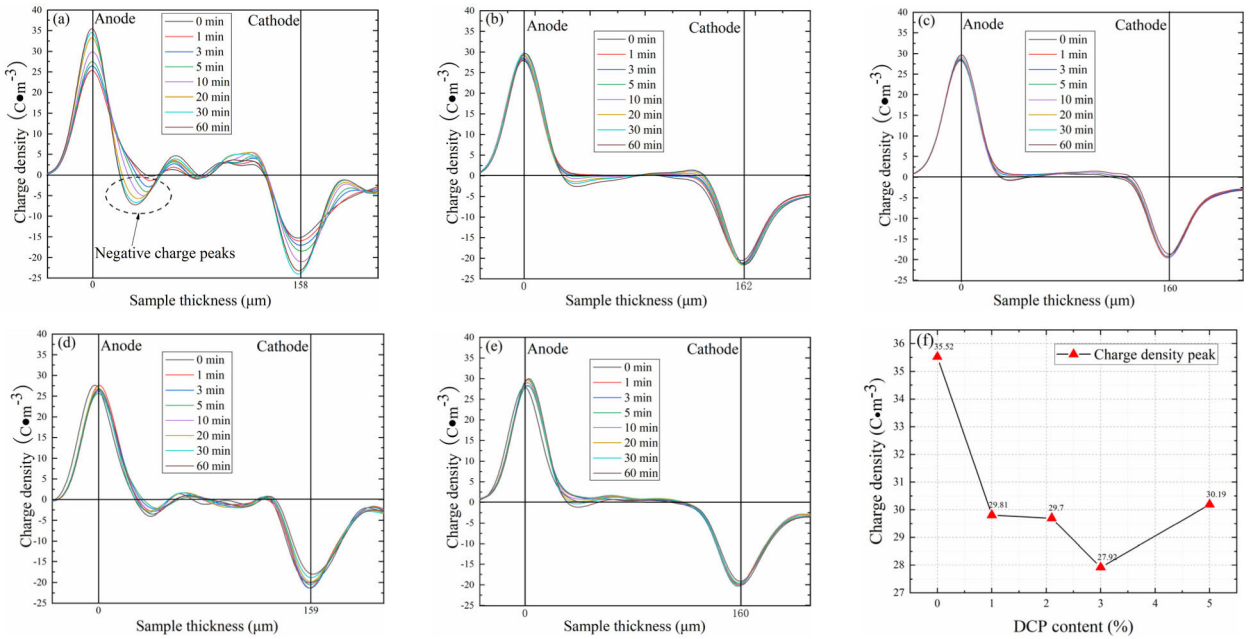

FIGURE 7. (a)-(e) Space charge density distributions of XLPE samples with different cross-linking agent contents in applied voltage experiment when thermal aging time is 15 days. (a) Pure LDPE. (b) 1.0% DCP. (c) 2.1% DCP. (d) 3.0% DCP. (e) 5.0% DCP. (f) Space charge density peak values at anode of XLPE samples with different cross-linking agent contents.

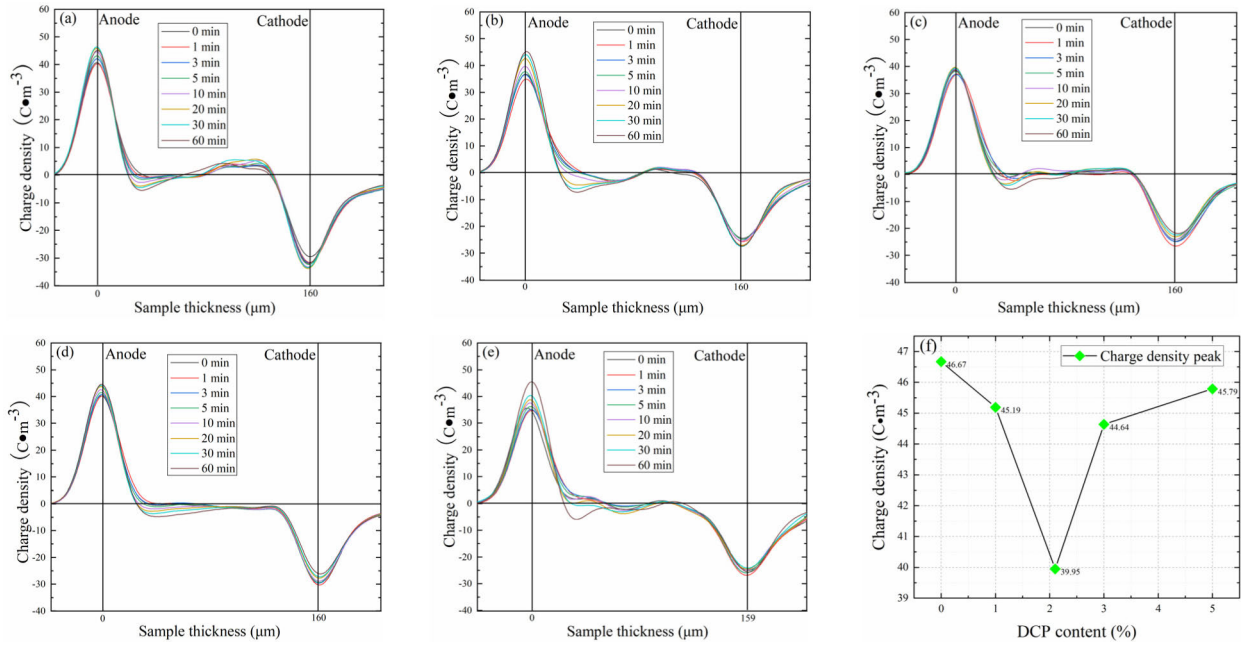

FIGURE 8. (a)-(e) Space charge density distributions of XLPE samples with different cross-linking agent contents in applied voltage experiment when thermal aging time is 30 days. (a) Pure LDPE. (b) 1.0% DCP. (c) 2.1% DCP. (d) 3.0% DCP. (e) 5.0% DCP. (f) Space charge density peak values at anode of XLPE samples with different cross-linking agent contents.

Figure 9 (a)-(e) shows space charge density distributions of XLPE samples with different cross-linking agent contents in applied voltage experiment when thermal aging time is 80 days. It can be seen from Figure 9 (a)-(e) that the fluctuation of space charge densities in these samples is very severe and space charge densities at the same position also fluctuate greatly when voltage application time is different, which indicates space charge distributions of samples aged for 80 days reach equilibrium for a long time. However, the fluctuation of space charge densities in unaged samples and samples at the early stage of thermal aging is relatively small, which indicates their charge distributions quickly reach

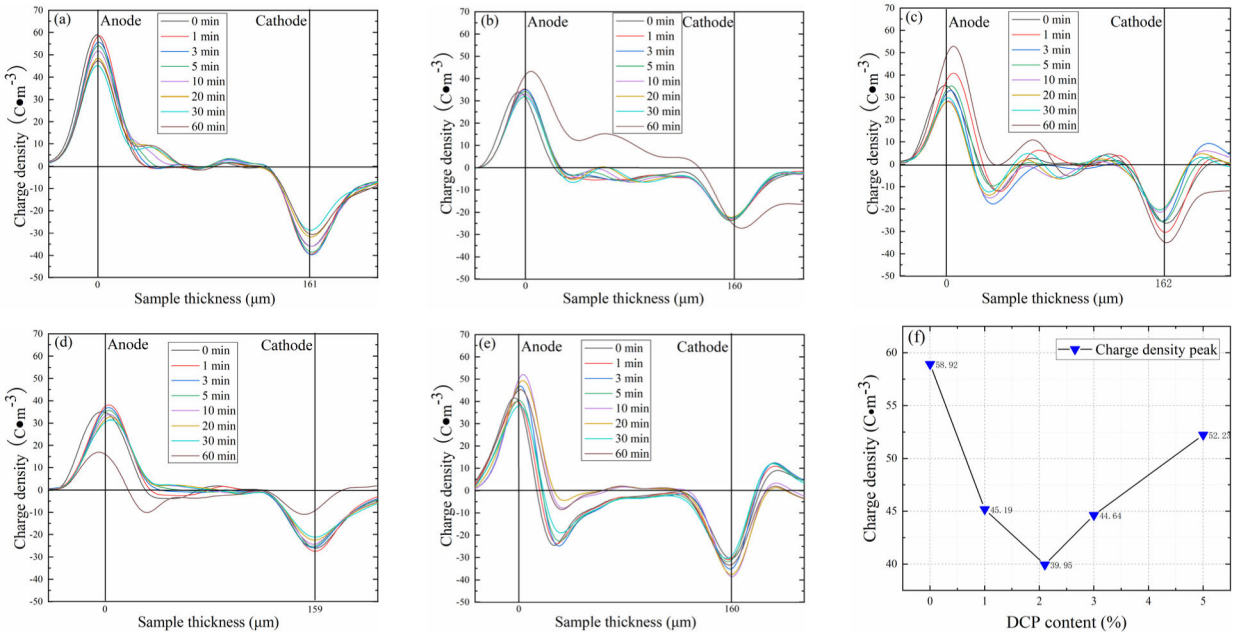

FIGURE 9. (a)-(e) Space charge density distributions of XLPE samples with different cross-linking agent contents in applied voltage experiment when thermal aging time is 80 days. (a) Pure LDPE. (b) 1.0% DCP. (c) 2.1% DCP. (d) 3.0% DCP. (e) 5.0% DCP. (f) Space charge density peak values at anode of XLPE samples with different cross-linking agent contents.

equilibrium. Space charge density peak values at anode are shown in Figure 9 (f). It can be seen from Figure 9 (f) that the value is minimized when DCP content is 2.1%, and these values are significantly increased compared with that of unaged samples. The most striking feature of samples aged for 80 days is that internal charge density of each sample is very large, and a large number of space charges are accumulated. The internal charge densities of XLPE samples aged for 15 and 30 days are less than that of pure LDPE sample, however, the internal charge density of pure LDPE sample aged for 80 days is smaller than that of XLPE samples aged for 80 days, and space charge distribution of pure LDPE sample tends to stabilize very quickly, while XLPE samples take longer to stabilize, which indicates the insulation performances of these samples have been deteriorated very seriously when thermal aging time is 80 days, and in the same case, the deterioration degree of XLPE is greater than that of pure LDPE.

In summary, the influence of thermal aging on space charge accumulation of XLPE with different cross-linking agent contents is as follows:

(a) Thermal aging can introduce negative charge traps into pure LDPE.

(b) Thermal aging can make space charges easier to inject and accumulate in pure LDPE and XLPE, but space charge densities in XLPE increase more rapidly as thermal aging time increases.

(c) At different thermal aging time, space charge density in XLPE with different cross-linking agent contents can decrease first and then increase in applied voltage experiment as DCP content increases.

B. INFLUENCE OF THERMAL AGING ON SPACE CHARGE DISSIPATION OF XLPE WITH DIFFERENT CROSS-LINKING AGENT CONTENTS

Figure 10 (a)-(e) shows space charge density distributions of XLPE samples with different cross-linking agent contents in voltage removal experiment when thermal aging time is 0 days. It can be seen from Figure 10 (a)-(e) that some charges trapped by charge traps inside unaged samples do not immediately disengage from charge traps and dissipates after the action of electric field strength, and positive and negative space charges can slowly dissipate as voltage removal time increases. Positive charge density peak values appear near the anode, and their values are shown in Figure 10 (f). It can be seen from Figure 10 (f) that these values have fluctuation as DCP content increases.

Figure 11 (a)-(e) shows space charge density distributions of XLPE samples with different cross-linking agent contents in voltage removal experiment when thermal aging time is 5 days. It can be seen from Figure 11 (a)-(e) that as DCP content increases, the number of charges trapped by charge traps inside these samples has a tendency to increase significantly, and the charge density of 5% DCP sample is the largest. In addition, there is a positive charge peak for each sample near the anode, and their values are shown in Figure 11 (f). Compared with space charge distributions of unaged samples, it can be seen from Figure 11 (a)-(e) that space charge density of each sample after thermal aging is greatly improved, and there are only residual positive charges in unaged samples, while there are a large number of residual negative charges in samples after thermal aging, which indicates thermal aging does introduce negative charge traps into pure LDPE.

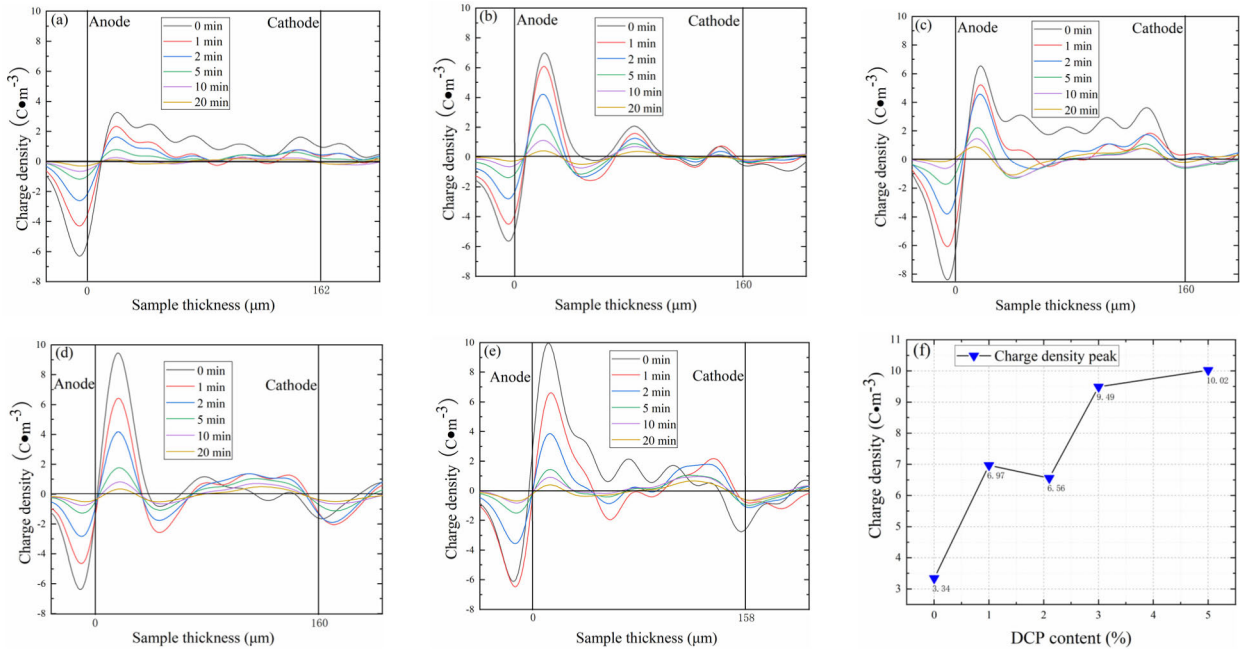

FIGURE 10. (a)-(e) Space charge density distributions of XLPE samples with different cross-linking agent contents in voltage removal experiment when thermal aging time is 0 days. (a) Pure LDPE. (b) 1.0% DCP. (c) 2.1% DCP. (d) 3.0% DCP. (e) 5.0% DCP. (f) Space charge density peak values near the anode of XLPE samples with different cross-linking agent contents.

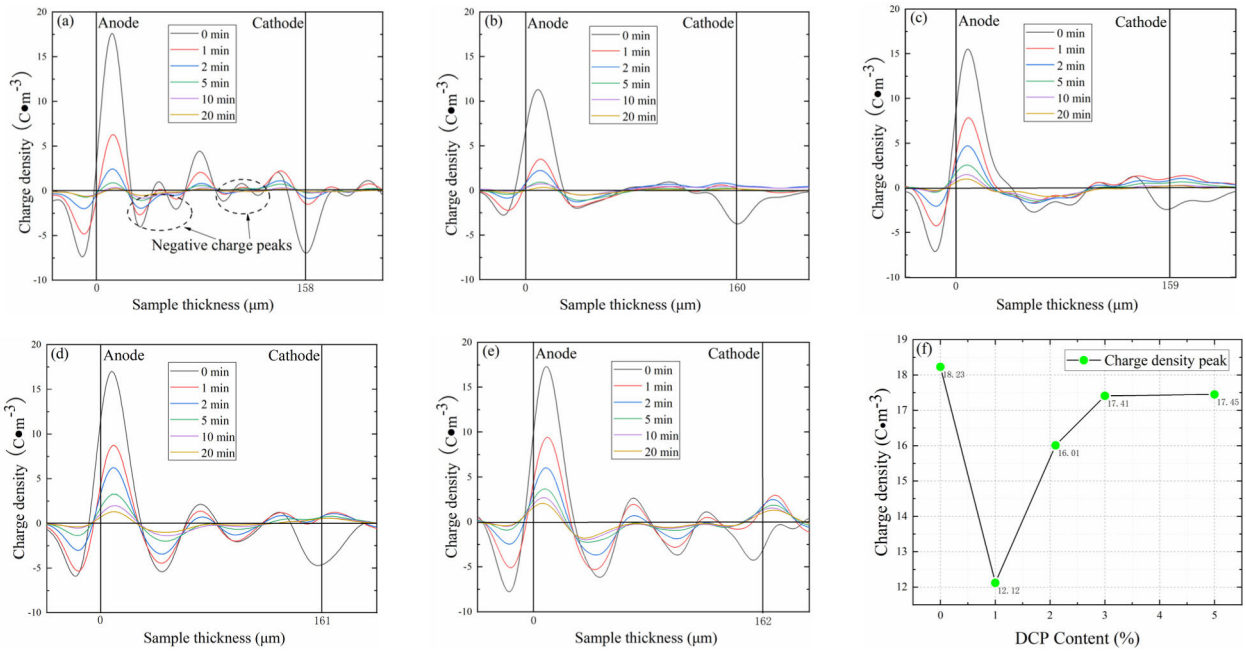

FIGURE 11. (a)-(e) Space charge density distributions of XLPE samples with different cross-linking agent contents in voltage removal experiment when thermal aging time is 5 days. (a) Pure LDPE. (b) 1.0% DCP. (c) 2.1% DCP. (d) 3.0% DCP. (e) 5.0% DCP. (f) Space charge density peak values near the anode of XLPE samples with different cross-linking agent contents.

Figure 12 (a)-(e) shows space charge density distributions of XLPE samples with different cross-linking agent contents in voltage removal experiment when thermal aging time is 15 days. It can be seen from Figure 12 (a)-(e) that there is still a positive charge peak for each sample near the anode, and their values are shown in Figure 12 (f). It can be seen from Figure 12 (f) that the value reaches maximum when DCP content is 3.0%. Because space charges trapped by shallow traps dissipate quickly after the voltage is removed, and the deeper charge traps, the slower dissipation speed of space

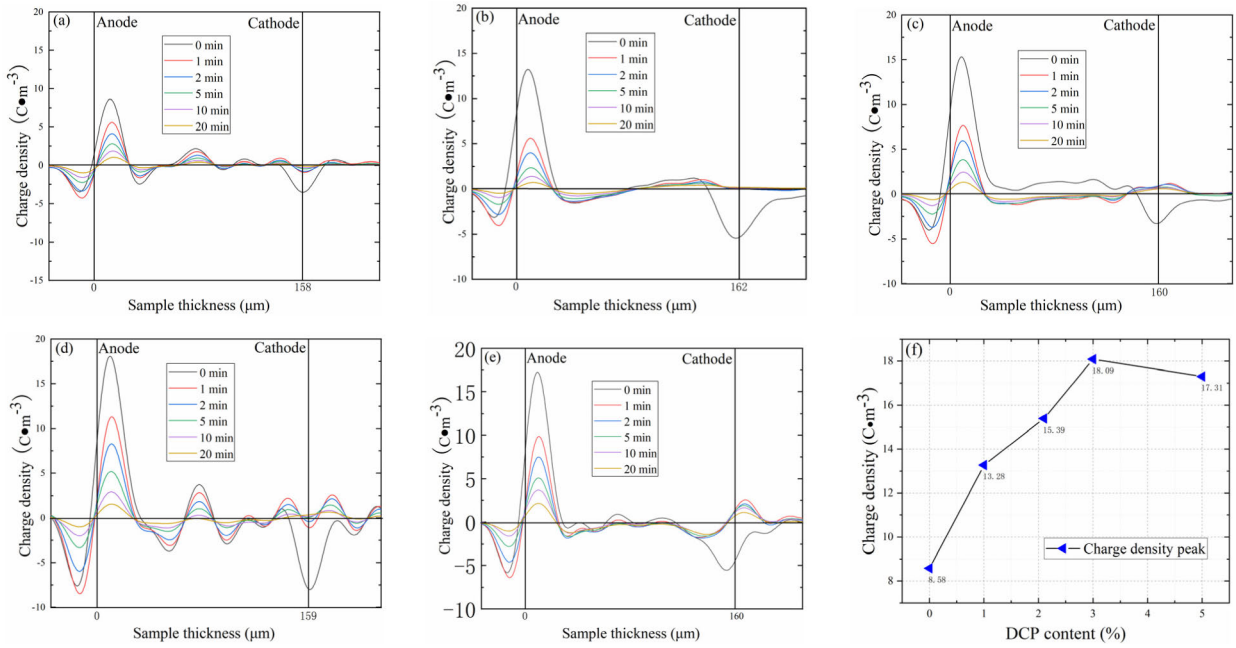

FIGURE 12. (a)-(e) Space charge density distributions of XLPE samples with different cross-linking agent contents in voltage removal experiment when thermal aging time is 15 days. (a) Pure LDPE. (b) 1.0% DCP. (c) 2.1% DCP. (d) 3.0% DCP. (e) 5.0% DCP. (f) Space charge density peak values near the anode of XLPE samples with different cross-linking agent contents.

charges. It can be seen by combining the charge distributions of applied and removed voltage experiments that the density of charge traps in pure LDPE is larger but the proportion of deep charge traps is smaller, however, the density of charge traps in XLPE is smaller but the proportion of deep charge traps is larger.

Figure 13 (a)-(e) shows space charge density distributions of XLPE samples with different cross-linking agent contents in voltage removal experiment when thermal aging time is 30 days. Similarly, there is a positive charge density peak for each sample near the anode, and their values are shown in Figure 13 (f). It can be seen from Figure 13 (f) that the value reaches maximum when DCP content is 1.0%. It can be seen from Figure 13 (a)-(e) that the number of charges trapped by charge traps inside samples aged for 30 days is significantly increased compared with that of unaged samples, which indicates thermal aging greatly increases the densities of deep charge traps in pure LDPE and XLPE. Besides, the increased proportion of charge trap density peak decreases first and then increases as DCP content increases, which indicates the increased rate of deep charge traps in aged samples decreases first and then increases as DCP content increases. It can be known that thermal aging can cause deep charge traps in these samples to increase at the slowest rate when DCP content is 3.0%. Space charges in applied voltage experiment are simultaneously trapped by deep and shallow charge traps, and residual charges in voltage removal experiment are mainly captured by deep charge traps [21], thus we can conclude thermal aging increases the densities of deep and shallow charge traps in XLPE with different cross-linking agent contents, and the increased proportion of deep charge traps decreases first and then increases (the increased proportion of shallow charge traps increases first and then decreases) as DCP content increases.

Figure 14 (a)-(e) shows space charge density distributions of XLPE samples with different cross-linking agent contents in voltage removal experiment when thermal aging time is 80 days. Similarly, there is still a positive charge density peak for each sample near the anode, and their values are shown in Figure 14 (f). It can be seen from Figure 14 (f) that the value reaches maximum when DCP content is 1.0%. In addition, it can be seen from Figure 14 (a)-(f) that space charge density peak value increases significantly compared with that of unaged samples and samples aged for 30 days, which indicates the number of deep charge traps in these samples has greatly increased when thermal aging time is 80 days, and the insulation performances of these samples have deteriorated very seriously.

Considering all space charge distributions of each sample, we can know more charges are accumulated in each sample after thermal aging in applied voltage experiment, and more charges trapped by charge traps are also left over after the voltage is removed. Because space charges in applied voltage experiment contain space charges trapped by shallow traps and deep traps and space charges in voltage removal experiment mainly contain space charges trapped by deep charge traps, thus we can conclude thermal aging results in a large increase in the number of shallow and deep charge traps in pure LDPE and XLPE.

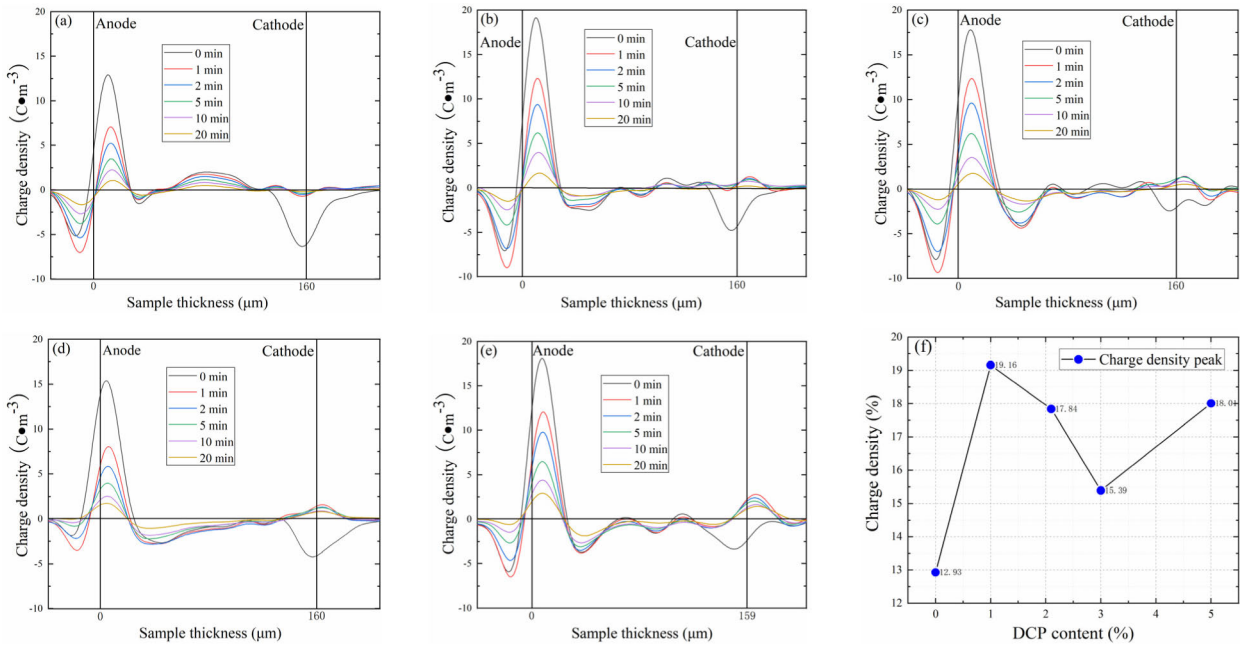

FIGURE 13. (a)-(e) Space charge density distributions of XLPE samples with different cross-linking agent contents in voltage removal experiment when thermal aging time is 30 days. (a) Pure LDPE. (b) 1.0% DCP. (c) 2.1% DCP. (d) 3.0% DCP. (e) 5.0% DCP. (f) Space charge density peak values near the anode of XLPE samples with different cross-linking agent contents.

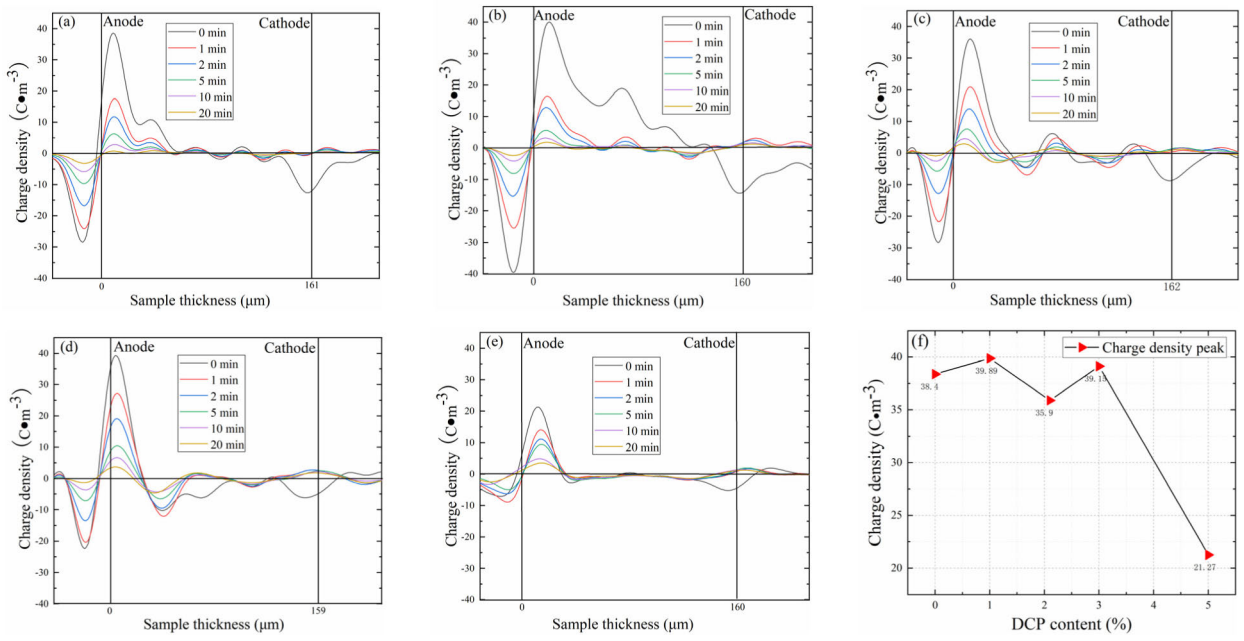

FIGURE 14. (a)-(e) Space charge density distributions of XLPE samples with different cross-linking agent contents in voltage removal experiment when thermal aging time is 80 days. (a) Pure LDPE. (b) 1.0% DCP. (c) 2.1% DCP. (d) 3.0% DCP. (e) 5.0% DCP. (f) Space charge density peak values near the anode of XLPE samples with different cross-linking agent contents.

In summary, the influence of thermal aging on space charge dissipation of XLPE with different cross-linking agent contents is as follows:

(a) Thermal aging can simultaneously increase the densities of deep and shallow charge traps in pure LDPE and XLPE, moreover, this growth rate is slower at the early stage of thermal aging, and the rate is faster at the end of thermal aging.

(b) As DCP content increases, the increased proportion of deep charge traps in XLPE with different cross-linking agent contents by thermal aging can show a trend of decreasing first and then increasing.

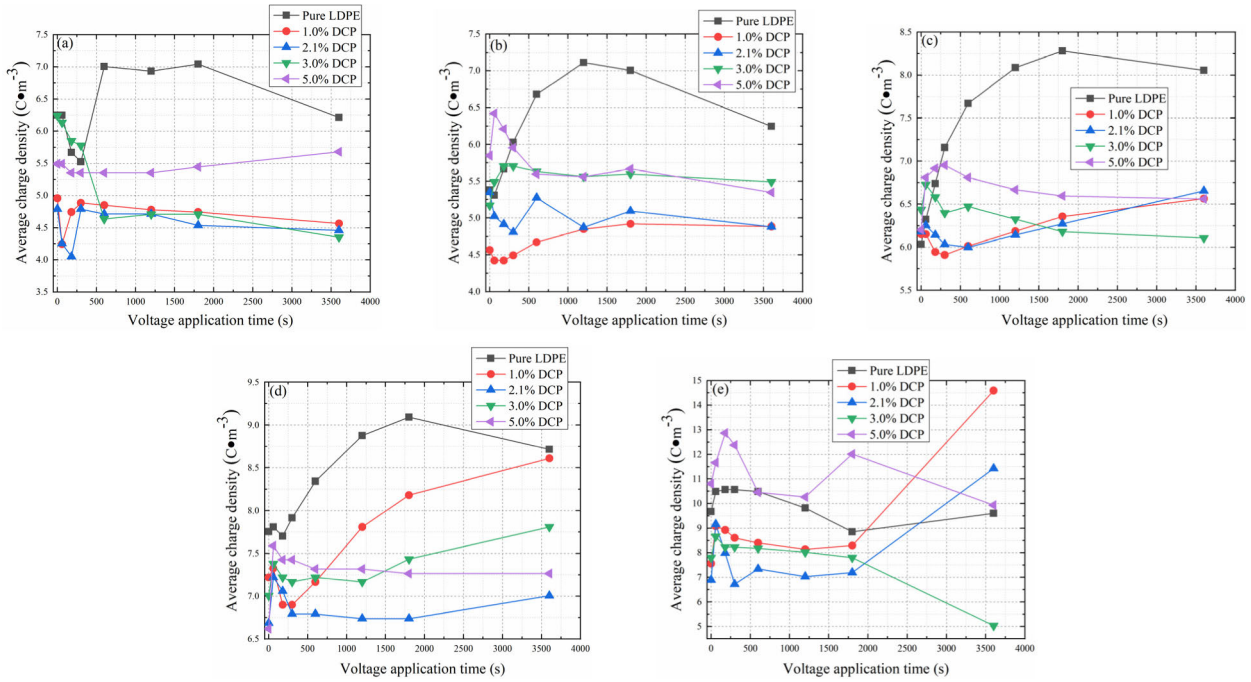

FIGURE 15. Average charge densities of samples with different thermal aging times in applied voltage experiment. (a) 0 days. (b) 5 days. (c) 15 days. (d) 30 days. (e) 80 days.

(c) At different thermal aging time, space charge densities in XLPE with different cross-linking agent contents can increase first and then decrease as DCP content increases in voltage removal experiment.

C. INFLUENCE OF THERMAL AGING ON AVERAGE CHARGE DENSITIES OF XLPE WITH DIFFERENT CROSS-LINKING AGENT CONTENTS

Figure 15 (a)-(e) shows average charge densities of samples with different thermal aging times in applied voltage experiment. It can be seen qualitatively from Figure 15 (a)-(e) that the injected and accumulated average charge density in each sample gradually increases as thermal aging proceeds. At the early stage of thermal aging (about 5 days), the average charge density of each sample is quickly stabilized in a short time. It can be seen from Figure 15 (a)-(e) that average charge densities when the time is 30min are not significantly different from that when the time is 60min, which indicates space charge distributions have basically reached a stable situation when the voltage is applied for 30min. However, it can also be seen from Figure 15 (a)-(e) that the average charge density of each sample fluctuates greatly at the end of thermal aging (about 80 days), additionally, there is still a large difference between average charge densities when the time is 30min and 60min, which indicates space charge distributions have not reached a stable situation when the voltage is applied for 30min. Besides, it can be also seen from Figure 15 (a)-(e) that space charge distributions greatly change during a period of 30min to 60min, which indicates the longer thermal aging time, the more intense space charge movement, and the longer it takes for space charge distributions to stabilize.

It can also be seen from Figure 15 (a)-(e) that average charge densities in these samples show a trend of decreasing first and then increasing as DCP content increases, and the lowest average charge densities of samples with different thermal aging times are not the same. The average charge density of 1.0% DCP sample is the lowest when thermal aging time is 5 days, and the average charge density of 2.1% DCP sample is also at a low level at the end of applied voltage experiment. Average charge densities of 1%, 2.1%, and 3% DCP samples are smaller when thermal aging time is 15 days. Average charge densities of 2.1% DCP samples are the lowest when thermal aging time is 30 days and 80 days. These indicate average charge densities of these samples have been relatively small when DCP content is 2.1% although thermal aging has increased average charge densities of all samples.

At the early stage of thermal aging (30 days ago), the average charge density of pure LDPE sample is significantly larger than that of XLPE samples during most of time, and the average charge density of 5.0% DCP sample exceeds that of pure LDPE to reach maximum when thermal time is 80 days, additionally, average charge densities of 1.0%, 2.1%, and 5.0% DCP samples are all greater than that of pure LDPE sample at the end of applied voltage experiment, which indicates space charge accumulation of these samples becomes easier as thermal aging time increases, and average charge densities of XLPE samples increase faster, namely, the electrical insulation performance of XLPE deteriorates

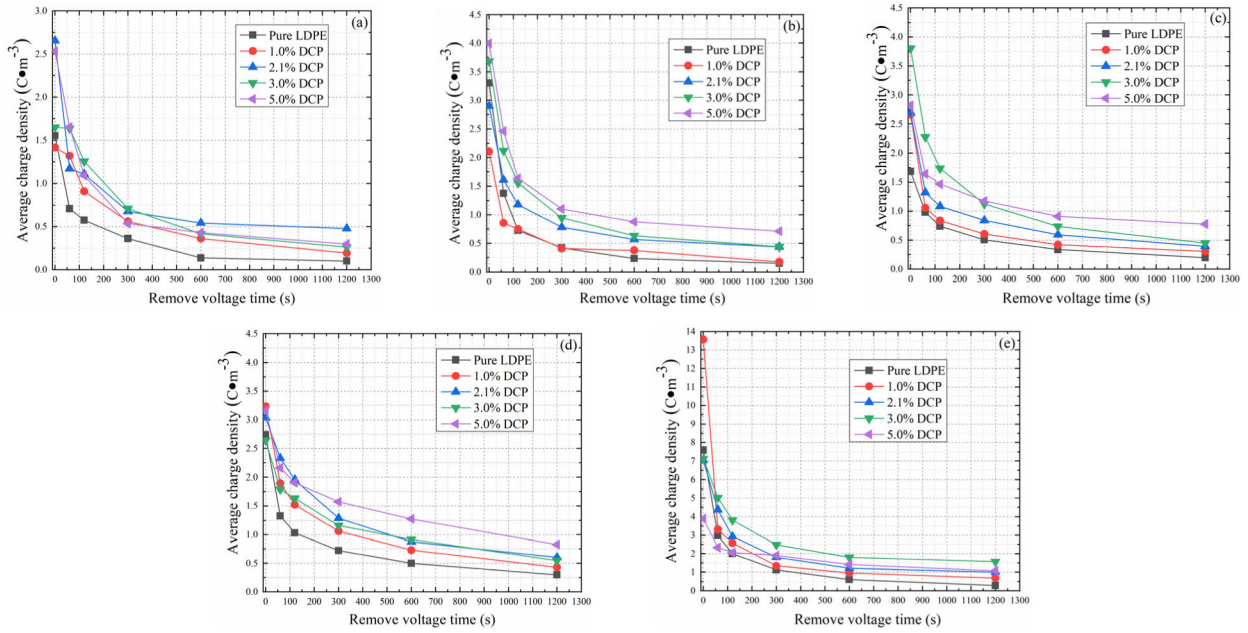

FIGURE 16. Average charge densities of samples with different thermal aging times in voltage removal experiment. (a) 0 days. (b) 5 days. (c) 15 days. (d) 30 days. (e) 80 days.

faster than that of pure LDPE when pure LDPE and XLPE are affected by thermal aging.

Besides, it can be seen from Figure 15 (a)-(e) that the average charge density of each sample gradually increases, and it increases faster and faster as thermal aging time increases, additionally, average charge density curves of samples aged for 5 days and unaged samples are basically at the same level, and average charge density curves of all samples have increased less in the period before thermal aging for 15 days, which indicates the increasing rate of average charge densities at the early stage of thermal aging are not very fast. The curves aged for 80 days are significantly increased compared with that aged for 30 days, which indicates the increasing rate of the average charge density of each sample at the end of thermal aging is very fast. It can be obviously seen from Figure 15 (a)-(e) that the fluctuation ranges of average charge density curves are small, and soon these curves enter a relatively stable stage at the early stage of thermal aging, however, the fluctuation range and duration of the average charge density curve of each sample is relatively long when thermal aging time is 80 days, which indicates thermal aging can cause these samples to accumulate more space charges and make space charges move faster.

In summary, thermal aging does make it easier for space charges to be injected and accumulated in pure LDPE and XLPE. And thermal aging also makes movement of space charges more intense, which greatly reduces the electrical insulation performance of pure LDPE and XLPE.

Figure 16 (a)-(e) shows average charge densities of samples with different thermal aging times in voltage removal experiment. It can be seen from Figure 16 (a)-(e) that space charges trapped by charge traps in each sample gradually decrease with time, and there is not much difference for space charges captured by charge traps in each sample at the early stage of thermal aging (30 days ago), however, space charge density of each sample increases significantly when thermal time is 80 days, and average charge densities of these samples show a trend of increasing first and then decreasing as DCP content increases, moreover, average charge densities of these samples increase as DCP content increases for most of time when thermal aging time is 5 days. It can be seen from Figure 16 (a)-(e) that there are some fluctuations of average charge densities in voltage removal experiment, and this can be mainly caused by the following two reasons: (a) Space charge decay rates of XLPE samples with different cross-linking agent contents are not the same as thermal aging time increases; (b) These samples themselves have a certain dispersion degree, and environmental condition during each experiment is also different.

D. MODEL OF SPACE CHARGE DISSIPATION

In order to quantitatively analyze the decay model of residual charges of each sample with time in voltage removal experiment, thereby obtaining the dissipation characteristics of space charges. Theoretical model of the average charge decay has been summed up in this article.

The expression is as follows:

$$\theta\,(\mathrm{t})\,\theta_0 + \beta \mathrm{e}^{-\frac{\mathrm{t}}{\lambda}} \tag{3}$$

In (3), θ(t) represents the average charge density which is the function of time t. θ_0 represents the number of residual charges when the average charge density decay tends to be stable. β represents the attenuation value of average charge

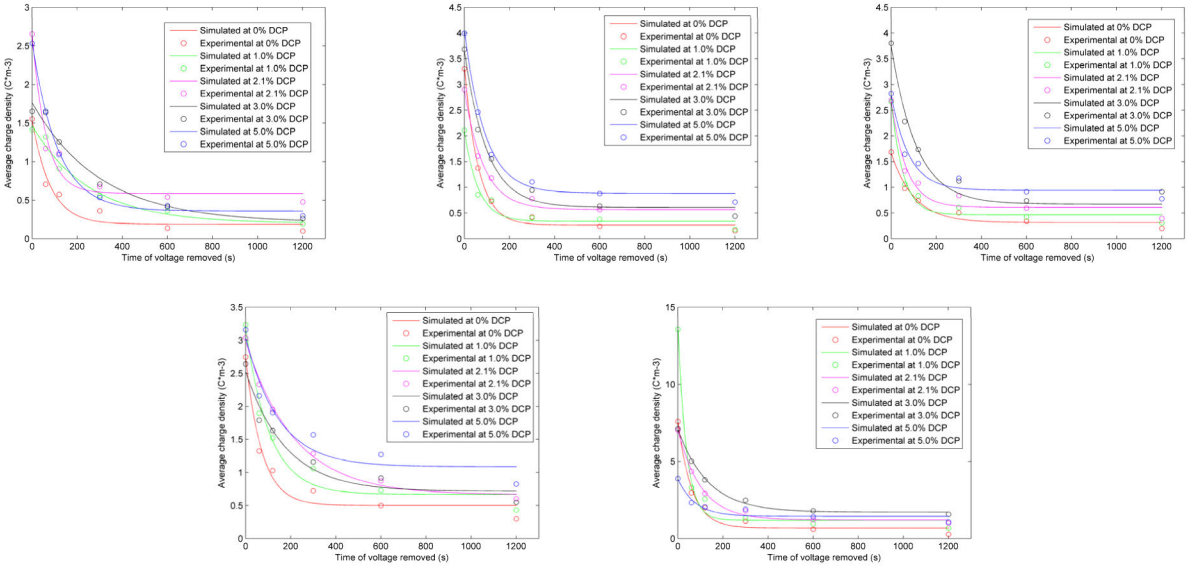

FIGURE 17. Comparisons between theoretical results obtained by theoretical model and real experimental data at different thermal aging times. (a) 0 days. (b) 5 days. (c) 15 days. (d) 30 days. (e) 80 days.

densities (the difference between initial value and stable value). λ represents a time constant of the average charge density decay.

In order to verify the correctness of theoretical model, theoretical results obtained by this theoretical model are compared with real experimental data. And the comparisons of different thermal aging times are shown in Figure 17 (a)-(e).

In Figure 17 (a), the values of R^2 from 0% DCP sample to 5.0% DCP sample respectively are 0.9640, 0.9795, 0.9672, 0.9770 and 0.9977. In Figure 17 (b), the values of R^2 from 0% DCP sample to 5.0% DCP sample respectively are 0.9954, 0.9678, 0.9878, 0.9878 and 0.9947. In Figure 17 (c), the values of R^2 from 0% DCP sample to 5.0% DCP sample respectively are 0.9757, 0.9794, 0.9635, 0.9803 and 0.9609. In Figure 17 (d), the values of R^2 from 0% DCP sample to 5.0% DCP sample respectively are 0.9723, 0.9683, 0.9945, 0.9564 and 0.9350. In Figure 17 (e), the values of R^2 from 0% DCP sample to 5.0% DCP sample respectively are 0.9855, 0.9897, 0.9950, 0.9964 and 0.9232.

It can be seen from these R^2 values that the variation discipline of theoretical results is in good agreement with the corresponding physical discipline of actual charge distributions, which indicates this theoretical model is effective for reflecting the dissipation of space charges in XLPE with different cross-linking agent contents of different thermal aging time. We can also perform preliminary theoretical analysis through this theoretical model [20]. For example, it means more charges remain in these samples after the voltage is removed when β is large, and it means the rate of charge dissipation in these samples is slow after this voltage is removed when λ is large, moreover, it can be used to infer these positions where more charges are accumulated or charge traps are deeper in these samples [20]–[25].

IV. MICRO INTERPRETATION

In fact, according to quantitative analysis based on average charge densities, the main influence of thermal aging on these samples with different thermal aging times is as follows:

(a) As thermal aging time increases, average charge densities increase in applied and removed voltage experiments, and the increased rate is slower at the early stage of thermal aging and faster at the end of thermal aging.

(b) At different thermal aging time, average charge densities decrease first and then increase as DCP content increases in applied voltage experiment, and average charge densities of 2.1% DCP samples are the smallest. Additionally, compared with pure LDPE, average charge densities of XLPE samples increase faster.

(c) At different thermal aging time, average charge densities of these samples show a trend of first increasing and then decreasing as DCP content increases in voltage removal experiment.

In fact, the reason for macro phenomena from previous researches [21]–[35] and the research results of this article is that thermal aging can increase the number of shallow charge traps of each sample, and the proportion of shallow charge traps increases first and then decreases as DCP content increases. For pure LDPE samples as shown in Figure 18 (a), when these samples are not aged, they are mainly dominated by shallow traps, while the densities of shallow charge traps are only increased after thermal aging, and then the number of space charges can gradually increase in voltage application and removal experiments.

However, for XLPE samples as shown in Figure 18 (b), the increase of shallow charge traps introduced by thermal aging can weaken the shielding effect [21]–[28]. Most charge traps are deep charge traps in unaged XLPE samples, and

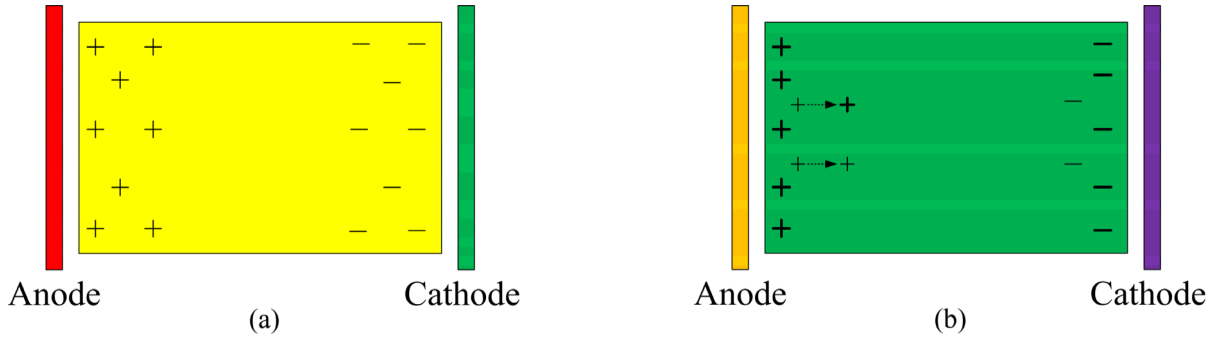

FIGURE 18. Schematic diagram for the principle of space charge injection and accumulation and dissipation of XLPE samples with different cross-linking agent contents after thermal aging (the thicker lines representing positive and negative charges, the deeper charge traps for trapping space charges). (a) Pure LDPE. (b) XLPE.

both shallow and deep traps near the sample surface can capture a certain number of space charges after thermal aging introduces a large number of shallow charge traps in applied voltage experiment, and at this time, these charges still have a shielding effect on two electrodes [27], [31]. However, space charges trapped by shallow charge traps are not stable at this time, and once these shallow charge traps are slightly disturbed, these charges can leave these traps and migrate further to deeper positions in these samples, and these charges may be captured by shallow or deep charge traps during migration. Thus these charges may stay there when they are captured by deep charge traps, while these charges are more likely to leave these charge traps and migrate deeper positions when they are captured by shallow charge traps, and then shallow and deep charge traps in deeper positions of these samples can capture more space charges.

At this time, due to the introduction of shallow charge traps, the shielding effect originally formed by space charges in deep charge traps on two electrodes can quickly weaken [34], which can cause threshold field strength of this material to decrease significantly as thermal aging time increases. Thus the number of space charges in these samples can increase significantly in voltage application and removal experiments.

Due to further increase of shallow charge traps, the shielding effect can rapidly weaken [33]–[34] when thermal aging time is 80 days, resulting in the rapid decrease of threshold field strength of XLPE samples. Thus space charge densities can significantly increase in voltage application and removal experiments. These shallow charge traps act like tunnels in the process [30]–[35], and although there are a large number of space charges trapped by deep charge traps near two electrodes to shield two electrodes, a large number of space charges can also accumulate inside these samples due to the transport of shallow charge traps, which can be called tunneling effect [28]–[35]. This is a great explanation for the change of space charge accumulation and dissipation of pure LDPE and XLPE after thermal aging from the perspective of micro-structure change of pure LDPE and XLPE.

V. CONCLUSION

In conclusion, in this article, a long-term thermal aging system is established to study the influence of thermal aging on space charge accumulation and dissipation of XLPE with different cross-linking agent contents, and an improved PEA method is used to measure space charge densities during voltage application and removal when thermal aging time respectively is 0, 5, 15, 30 and 80 days due to higher accuracy. And experimental results indicate thermal aging can introduce negative charge traps into pure LDPE and make space charges easier to inject and accumulate in pure LDPE and XLPE, but space charge densities in XLPE increase more rapidly as thermal aging time increases, and thermal aging can simultaneously increase densities of deep and shallow charge traps in pure LDPE and XLPE, moreover, this growth rate is slower at the early stage of thermal aging and faster at the end of thermal aging, additionally, the increased proportion of deep charge traps in pure LDPE and XLPE by thermal aging can show a trend of decreasing first and then increasing as DCP content increases, and at different thermal aging times, as DCP content increases, space charge densities in pure LDPE and XLPE can decrease first and then increase during voltage application while that can increase first and then decrease during voltage removal, and the quantitative analysis of average charge densities has also proved these conclusions. In addition, we have also explained the change of space charge accumulation and dissipation of pure LDPE and XLPE after thermal aging from the perspective of micro-structure change of pure LDPE and XLPE through the quantitative analysis of average charge densities. Besides, theoretical model of the average charge decay has also been summed up, and this model can perfectly reflect the dissipation characteristics of space charges in XLPE with different cross-linking agent contents of different thermal aging time.

REFERENCES

[1] Z. Y. Li and G. Chen, "Space charge in thermally aged polyethylene and its electrical performance," *Mater. Res. Express*, vol. 6, no. 3, pp. 1–12, Mar. 2019.

[2] D. Manas, M. Manas, A. Mizera, P. Stoklasek, J. Navratil, S. Sehnalek, and P. Drabek, "The high density polyethylene composite with recycled radiation cross-linked filler of rHDPEx," *Polym.*, vol. 10, no. 12, pp. 1–13, Dec. 2018.
[3] I. Plesa, P. V. Notingher, S. Schlogl, C. Sumereder, and M. Muhr, "Properties of polymer composites used in high-voltage applications," *Polym.*, vol. 8, no. 5, pp. 1–63, May 2016.
[4] G. Li, J. Wang, W. Han, Y. Wei, and S. Li, "Influence of temperature on charge accumulation in low-density polyethylene based on depolarization current and space charge decay," *Polymer*, vol. 11, no. 4, pp. 1–10, Apr. 2019.
[5] W. Choo, G. Chen, and S. G. Swingler, "Electric field in polymeric cable due to space charge accumulation under DC and temperature gradient," *IEEE Trans. Dielectr. Electr. Insul.*, vol. 18, no. 2, pp. 596–606, Apr. 2011.
[6] M. Fu, L. Dissado, G. Chen, and J. Fothergill, "Space charge formation and its modified electric field under applied voltage reversal and temperature gradient in XLPE cable," *IEEE Trans. Dielectr. Electr. Insul.*, vol. 15, no. 3, pp. 851–860, Jun. 2008.
[7] D. Min, W. Wang, and S. Li, "Numerical analysis of space charge accumulation and conduction properties in LDPE nanodielectrics," *IEEE Trans. Dielectr. Electr. Insul.*, vol. 22, no. 3, pp. 1483–1491, Jun. 2015.
[8] Y. Sekii and T. Maeno, "Generation and dissipation of negative heterocharges in XLPE and EPR," *IEEE Trans. Dielectr. Electr. Insul.*, vol. 16, no. 3, pp. 668–675, Jun. 2009.
[9] G. Teyssedre and C. Laurent, "Charge transport modeling in insulating polymers: From molecular to macroscopic scale," *IEEE Trans. Dielectr. Electr. Insul.*, vol. 12, no. 5, pp. 857–875, Oct. 2005.
[10] B. Vissouvanadin, S. L. Roy, G. Teyssedre, C. Laurent, I. Denizet, M. Mammeri, and B. Poisson, "Impact of concentration gradient of polarizable species on the electric field distribution in polymeric insulating material for HVDC cable," *IEEE Trans. Dielectr. Electr. Insul.*, vol. 18, no. 3, pp. 833–839, Jun. 2011.
[11] D. Fabiani, G. Montanari, L. Dissado, C. Laurent, and G. Teyssedre, "Fast and slow charge packets in polymeric materials under DC stress," *IEEE Trans. Dielectr. Electr. Insul.*, vol. 16, no. 1, pp. 241–250, Feb. 2009.
[12] G. Mazzanti, G. C. Montanari, and J. M. Alison, "A space-charge based method for the estimation of apparent mobility and trap depth as markers for insulation degradation-theoretical basis and experimental validation," *IEEE Trans. Dielectr. Electr. Insul.*, vol. 10, no. 2, pp. 187–197, Apr. 2003.
[13] F. Rogti, A. Mekhaldi, and C. Laurent, "Space charge behavior at physical interfaces in cross-linked polyethylene under DC field," *IEEE Trans. Dielectr. Electr. Insul.*, vol. 15, no. 5, pp. 1478–1485, Oct. 2008.
[14] F. Rogti, "Space charge dynamic at the physical interface in cross-linked polyethylene under DC field," *IEEE Trans. Dielectr. Electr. Insul.*, vol. 18, no. 3, pp. 888–899, Jun. 2011.
[15] T. Tanaka, A. Bulinski, J. Castellon, M. Frechette, S. Gubanski, J. Kindersberger, G. C. Montanari, M. Nagao, P. Morshuis, Y. Tanaka, S. Pelissou, A. Vaughan, Y. Ohki, C. W. Reed, S. Sutton, and S. J. Han, "Dielectric properties of XLPE/SiO_2 nanocomposites based on CIGRE WG D1.24 cooperative test results," *IEEE Trns. Dielectr. Electr. Insul.*, vol. 18, no. 5, pp. 1484–1517, Oct. 2011.
[16] C. Stancu, P. V. Notingher, and P. Notingher, "Influence of space charge related to water trees on the breakdown voltage of power cable insulation," *J. Electrostatics*, vol. 71, no. 2, pp. 145–154, Apr. 2013.
[17] T. Takada, "Acoustic and optical methods for measuring electric charge distributions in dielectrics," *IEEE Trans. Dielectr. Electr. Insul.*, vol. 6, no. 5, pp. 519–547, Oct. 1999.
[18] G. Chen, Y. L. Chong, and M. Fu, "Calibration of the pulsed electroacoustic technique in the presence of trapped charge," *Meas. Sci. Technol.*, vol. 17, no. 7, pp. 1974–1980, Jul. 2006.
[19] N. Hozumi, H. Suzuki, T. Okamoto, K. Watanabe, and A. Watanabe, "Direct observation of time-dependent space charge profiles in XLPE cable under high electric fields," *IEEE Trans. Dielectr. Electr. Insul.*, vol. 1, no. 6, pp. 1068–1076, Dec. 1994.
[20] S. C. Wang, Q. Zhou, R. J. Liao, L. Xing, N. C. Wu, and Q. Jiang, "The impact of cross-linking effect on the space charge characteristics of cross-linked polyethylene with different degrees of cross-linking under strong direct current electric field," *Polymer*, vol. 11, no. 7, pp. 1–28, Jul. 2019.
[21] F. Tian, W. Bu, L. Shi, C. Yang, Y. Wang, and Q. Lei, "Theory of modified thermally stimulated current and direct determination of trap level distribution," *J. Electrostatics*, vol. 69, no. 1, pp. 7–10, Feb. 2011.
[22] M. Meunier and N. Quirke, "Molecular modeling of electron trapping in polymer insulators," *J. Chem. Phys.*, vol. 113, no. 1, pp. 369–376, Jul. 2000.
[23] M. Meunier, N. Quirke, and A. Aslanides, "Molecular modeling of electron traps in polymer insulators: Chemical defects and impurities," *J. Chem. Phys.*, vol. 115, no. 6, pp. 2876–2881, Aug. 2001.
[24] L. Qingquan, T. Fuqiang, Y. Chun, H. Lijuan, and W. Yi, "Modified isothermal discharge current theory and its application in the determination of trap level distribution in polyimide films," *J. Electrostatics*, vol. 68, no. 3, pp. 243–248, Jun. 2010.
[25] K. J. Kao, S. S. Bamji, and M. M. Perlman, "Thermally stimulated discharge current study of surface charge release in polyethylene by corona generated excited molecules, and the crossover phenomenon," *J. Appl. Phys.*, vol. 50, no. 12, pp. 8181–8185, Dec. 1979.
[26] F. Q. Tian, Q. Q. Lei, X. Wang, and Y. Wang, "Effect of deep trapping states on space charge suppression in polyethylene/ZnO nanocomposite," *Appl. Phys. Lett.*, vol. 99, no. 14, pp. 1–3, Oct. 2011.
[27] Z. K. Lu, "Study on transient behavior of space charge in polyethylene materials for high voltage DC cables," M.S. thesis, Dept. Electron. Eng., Zhengzhou Univ., Zhengzhou, China, 2019.
[28] L.-J. He, L. Dai, C. Yang, F.-Q. Tian, L. Zhao, J.-L. Cao, X. Wang, and Q.-Q. Lei, "Study on deep trap states in polymers by photo-stimulated discharge based on the OPO laser," *Modern Phys. Lett. B*, vol. 24, no. 18, pp. 1933–1941, Jul. 2010.
[29] O. W. Liu, "Effect of thermal aging on electrical and mechanical properties of HVDS cable cross-linked polyethylene," M.S. thesis, Dept. Electron. Eng., North China Electric Power Univ., Beijing, China, 2018.
[30] Y. Qin, "Effect of thermal aging on dielectric properties of nano-CB/XLPE composite insulation materials," M.S. thesis, Dept. Electron. Eng., Harbin Univ., Harbin, China, 2018.
[31] H. Boukhari and F. Rogti, "Simulation of space charge dynamic in polyethylene under DC continuous electrical stress," *J. Electron. Mater.*, vol. 45, no. 10, pp. 5334–5340, Oct. 2016.
[32] F. Q. Tian, "Investigation on the trap characteristics and electrical properties of polyethylene based nanocomposite," Ph.D. dissertation, Dept. Elect. Eng., Beijing Jiaotong Univ., Beijing, China, 2012.
[33] T. Tanaka and A. Greenwood, "Effects of charge injection and extraction on tree initiation in polyethylene," *IEEE Trans. Power App. Syst.*, vols. PAS–97, no. 5, pp. 1749–1759, Sep. 1978.
[34] W. Bu, J. Yin, F. Tian, G. Li, and Q. Lei, "Effect of corona ageing on the structure changes of polyimide and polyimide/Al_2O_3 nanocomposite films," *J. Electrostatics*, vol. 69, no. 3, pp. 141–145, Jun. 2011.
[35] N. Ueno, K. Sugita, K. Seki, and H. Inokuchi, "Low-energy electron transmission and secondary-electron emission experiments on crystalline and molten long-chain alkanes," *Phys. Rev. B, Condens. Matter*, vol. 34, no. 9, pp. 6386–6393, Nov. 1986.

SHUCHAO WANG was born in Suihua, Heilongjiang, China, in 1995. He received the B.S. degree in electrical engineering from the Harbin University of Science and Technology, Harbin, Heilongjiang, in 2018. He is currently pursuing the M.S. degree in electrical engineering with Chongqing University, Chongqing, China.

QUAN ZHOU is currently a Full Professor and a Ph.D. Tutor with the Electrical Engineering School, Chongqing University, Chongqing, China. He is mainly involved in the application of basic research in the fields of electrical equipment insulation monitoring and fault diagnosis theory and technology, safety assessment of new energy power equipment, intelligent distribution network optimization, and fault diagnosis. He is also a member of the IEEE Dielectrics and Electrical Insulation Society (DEIS).

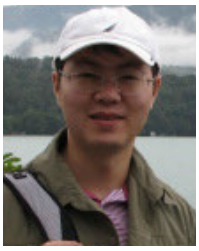

JIAN LI (Senior Member, IEEE) is currently a Full Professor and a Ph.D. Tutor with the Electrical Engineering School, Chongqing University, Chongqing, China. He is mainly involved in the research of intelligent transmission and transformation equipment and new types of electrical insulation materials. He was a recipient of the National Outstanding Youth Science Foundation of China, a specially-appointed professor of Bayu Scholars at the Chongqing of China, and a new century excellent talent of the Ministry of Education of China. He has also been an Associate Editor of the IEEE TRANSACTIONS ON DIELECTRICS AND ELECTRICAL INSULATION (DEI), the Director of the IEEE Dielectrics and Electrical Insulation Society (DEIS) and the IEEE Conference on Electrical Insulation and Dielectric Phenomena (CEIDP), and a member of the CIGRE working group.

RUIJIN LIAO is currently a Full Professor and a Ph.D. Tutor with the Electrical Engineering School, Chongqing University, Chongqing, China. He is also the Vice Principal of Chongqing University. He is also a Distinguished Professor with Changjiang Scholars of China, a recipient of the National Outstanding Youth Fund of China, the Leader of the Natural Fund's Innovative Research Group of High-voltage transmission and distribution equipment safety theory and technology of China, a cross-century talented person from the Ministry of Education of China, and a Distinguished Professor of Two River Scholars in Chongqing of China. He also serves as a member of GIGRE SC-C4 and CIGRE China National Committee.

NENGCHENG WU received the M.S. degree in electrical engineering from Chongqing University, Chongqing, China, in 2013. He is currently an Employee of Deyang Electric Power Supply Company, State Grid Corporation of China.

YONG LI was born in Zhaotong, Yunnan, China, in 1995. He received the B.S. degree in electrical engineering from Northeastern University, Shenyang, Liaoning, China, in 2019. He is currently pursuing the M.S. degree in electrical engineering with Chongqing University, Chongqing, China.

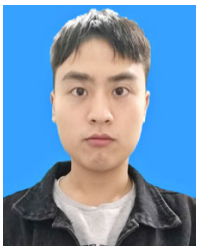

MINGHAO CHEN was born in Deyang, Sichuan, China, in 1997. He received the B.S. degree in electrical engineering from the China University of Mining and Technology, Xuzhou, Jiangsu, China, in 2015. He is currently pursuing the M.S. degree in electrical engineering with Chongqing University, Chongqing, China.